High-speed Weighing Using Impact on Load Cells

Andrew Gilman

Institute of Information Sciences and Technology
Massey University
Palmerston North, New Zealand
a.gilman@massey.ac.nz

Donald G. Bailey

Institute of Information Sciences and Technology
Massey University
Palmerston North, New Zealand
d.g.bailey@massey.ac.nz

Abstract—**Many techniques employed in current weighing systems rely on the step response of one or a number of force transducers for making measurements. However, force transducers can have significant settling time, which limits the maximum rate at which measurements can be made. This paper presents a method of weight measurement that utilizes the impact of an object on a load cell. The impact impulse can be approximated by the Dirac delta function and hence the output resembles the impulse response. The size of the impact impulse and the weight of the object can be found from this impulse response. Signal processing is used to eliminate the long oscillatory response of the force transducer, allowing the measurements to be made at a much higher rate.**

I. INTRODUCTION

A. Motivation

In today's highly automated industrial world, in-process electronic weighing systems play an important role in a number of essential areas such as quality control, sorting, and grading. As processing speeds continue to grow, the need for high-speed weighing methods becomes increasingly important.

A large number of current industrial high-speed weighing systems rely on the step response of a force transducer to determine the weight of a part of a moving conveyor belt including any items on the belt at the time. This creates a number of problems inherent to the method, in particular the long settling time of force transducers and vibration created by mechanical parts of the conveyor. It is possible to use adaptive filtering to decrease the effect of external vibration [1], but benefits can be gained by eliminating vibration by making the weighing table motionless. Then, loading and unloading of items to record the step response becomes problematic.

In this paper, an alternative method to using the transducer step response will be considered. The most common force transducer type is a load cell.

B. System Model

A typical load cell system is comprised of three subsystems: the load cell, the strain gauge, and the load cell amplifier. The strain gauge and the load cell are actually a single physical device, but will be considered separately for clarity. The input to the system is a force applied onto the load cell, and the output is a voltage produced by the load cell amplifier.

1) Load Cell: A typical load cell contains two characteristic components: a spring element and one or more strain gauges. The function of the spring element is two-fold. It serves as the reaction for the applied load and focuses the effect of the load into an isolated, uniform strain-field. In a cantilever load cell, the spring element is a part of the cantilever itself – the beam stores elastic potential energy as the live end is deflected from the equilibrium position.

As the angle of deflection is small, the live end of the load cell can be assumed to travel linearly along the vertical axis. A simple model of the load cell can be represented by a mass M (equivalent mass of the live end of the load cell) attached to a mass-less spring with spring constant k_s. As a load is applied to the load cell, a counteracting force produced by the spring due to an offset x from equilibrium is defined by Hooke's law as

$$f_s = -k_s x$$
.

This would be sufficient to model the load cell in a static equilibrium, but in analysing the dynamic characteristics, it is important to take into account the damping. To simplify the model, viscous damping is assumed, where the damping force is proportional to the velocity: $f_D = -k_D \dot{x}$ (k_D is the damping constant). Fig. 1 shows the free-body-diagram of the forces acting on the live end of the load cell.

Newton's 2nd law can be used to find the equation representing the movement of the live end of the load cell in response to an external excitation force $f(t)$:

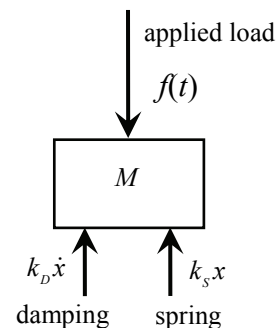$$M\ddot{x}(t) = f(t) - k_s x(t) - k_D \dot{x}(t). \qquad (1)$$

Figure 1.   Free-body-diagram of the live end of the load cell.

The system response of the load cell can be found by rearranging the Laplace transform of (1) (assuming zero initial conditions):

$$H_{LC}(s) = \frac{X(s)}{F(s)} = \frac{1/M}{s^2 + \frac{k_D}{M}s + \frac{k_S}{M}} = \frac{1/M}{(s + \sigma_L)^2 + \omega^2}, \quad (2)$$

where σ_L and ω (for an underdamped response) are given by:

$$\sigma_L = \frac{k_D}{2M},$$
$$\omega = \sqrt{\frac{k_S}{M} - \frac{k_D^2}{4M^2}}. \qquad (3)$$

2) Strain Gauges: The deflection of the cantilever is measured using strain gauges – the bending stretches the strain gauge elements, changing their resistance. The foil strain gauge is the most widely used type. The change in resistance of such a gauge is relatively small. A typical way of detecting this change and converting it into voltage is the use of a Wheatstone bridge. The bridge will normally be balanced while the gauge is unstrained; the bridge output, as the gauge is then strained, can provide a sensitive and reasonably linear indication over a wide range of strain.

For a Wheatstone bridge consisting of four strain gauges and for small deflections, the differential voltage is approximately proportional to the strain. The system response of the bridge inside the operational region is therefore a constant:

$$H_{SG} = B . \qquad (4)$$

3) Instrumentation Amplifier: To ensure good linearity, the load cell output at full-scale deflection is on order of millivolts; hence, an amplifier is required to increase the signal before it can be processed. Instrumentation amplifiers are often employed because of their low drift, low noise, high gain, and high common mode rejection ratio (CMRR) characteristics.

The amplifier system response often possesses a first order low-pass characteristic:

$$H_A = \frac{G}{s + \sigma_A}, \qquad (5)$$

where G is the amplifier gain and σ_A is the cut-off frequency.

4) Combined System: The sub-system responses (2), (4), and (5) can be multiplied together to get the combined system response of the load cell-amplifier system:

$$H(s) = \frac{GB/M}{(s + \sigma_A)((s + \sigma_L)^2 + \omega^2)} . \qquad (6)$$

The impulse response of the system can be found by taking the inverse Laplace transform of (6):

$$h(t) = \frac{GB}{MR}\left(e^{-\sigma_A t} - \frac{\sqrt{R}}{\omega} e^{-\sigma_L t} \cos(\omega t + \theta) \right). \qquad (7)$$

where R and θ are given by:

$$R = (\sigma_L - \sigma_A)^2 + \omega^2,$$
$$\theta = \tan^{-1}\frac{\sigma_L - \sigma_A}{\omega}. \qquad (8)$$

C. Impact Impulse for Weighing

Normally, the system described above would be used to measure the weight of an object placed onto the load cell by evaluating the step response, or the difference in the output before the object has been placed and after. After the transients have decayed, the step response output is proportional to the input load.

The proposed method of high-speed weighing uses a similar set-up, but the objects to be weighed are dropped onto the load cell. An impact occurs when the object comes into contact with the live end of the load cell, where the load cell and the object exert relatively large forces on each other, but only for a short time. Although complete understanding of the impact requires an extensive analysis of the contact forces, the stresses, and the deformations of the colliding bodies, the principle of conservation of momentum can be used to obtain a good approximation to the impact event.

A number of simplifying assumptions can be made to keep the analysis straightforward. The object is assumed to rebound and travel in the opposite direction after the collision with the load cell, as illustrated in Fig. 2. The velocity of separation is assumed to be a fixed fraction of the velocity of approach and the initial velocity of the load cell is assumed to be negligible:
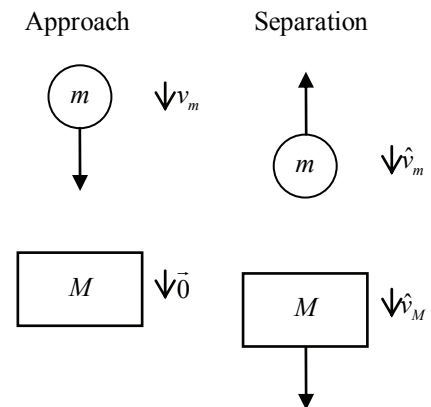

Figure 2.   An object with mass *m* is approaching the live end of the load cell with live end equivalent mass *M*. The two collide and separate.

$$\hat{v}_M - \hat{v}_m = e(v_m - 0). \qquad (9)$$

where e is the coefficient of restitution.

The impact interval is assumed sufficiently short, so that during the impact the following statements are true.

- The effect of gravity on the velocity of the object impacting the load cell is negligible.

- The effect of restoring and damping forces on the velocity of the load cell is negligible.

- The position or orientation of the object or the load cell has no significant change during impact.

The linear momentum is being conserved, as the system is isolated and closed. Conservation of the linear momentum gives:

$$mv_m + 0 = m\hat{v}_m + M\hat{v}_M. \qquad (10)$$

Solving (9) and (10) for final velocities gives:

$$\hat{v}_m = \frac{(m - eM)}{m + M} v_m, \qquad (11)$$

$$\hat{v}_M = \frac{m(1 + e)}{m + M} v_m. \qquad (12)$$

The impulse J, due to the impact force acted upon the live end of the load cell by the object is equal to the change in momentum of the load cell:

$$J = M\hat{v}_M = \frac{mMv_m}{m + M}(1 + e). \qquad (13)$$

M is constant for any given configuration of the apparatus. The coefficient of restitution is an index of the degree to which bodies recover from deformation due to a collision [2]. It is frequently considered a constant for given geometries and a given combination of contacting materials, but in reality, it also depends on the impact velocity and approaches unity as the impact velocity approaches zero. However, if the impact velocity is above a certain threshold, the restitution coefficient can be considered to be independent of it.

Rearranging (13) to give the mass of the object being measured as a function of the impulse J and the impact velocity v_m:

$$m(J, v_m) = \frac{MJ}{M(1 + e)v_m - J}. \qquad (15)$$

Since the bandwidth of the system is much smaller than the bandwidth of the impulse, the impact impulse can be approximated by a Dirac delta function $\delta(t)$ scaled by J, then the system output is a scaled impulse response, $Jh(t)$. This means that J can be found from the load cell output. Hence, if we can measure the impact velocity and the output of the system, we can determine the mass of the dropped object, given the above assumptions are satisfied.

D. Impact Velocity

A number of approaches can be used to determine the velocity of a falling object. One simple approach is to measure the time t_T it takes for the object to fall a certain distance d prior to the impact. Then, if we assume that the object is being accelerated solely by the force of gravity, the impact velocity becomes a function of t_T and d:

$$v_m(t_T, d) = \frac{d}{t_T} + \frac{1}{2} gt_T. \qquad (16)$$

E. High-speed Weighing Using Digital Processing

In order to process the load cell signal using a digital computer, the signal has to be sampled and digitized. After sampling (7), the impulse response becomes:

$$h[n] = \frac{GB}{MR}\left(e^{-\sigma_A nT} - \frac{\sqrt{R}}{\omega} e^{-\sigma_L nT} \cos\left(\omega nT + \theta\right) \right), \qquad (17)$$

where T is the sampling period and n is the sample number. Equation (14) is the transfer function and can be found by taking the z-transform of (17).

The denominator of the transfer function indicates three distinct poles: a single real pole that originates from the amplifier response and a pair of complex conjugate-symmetric poles that originates from the load cell. This pair of poles is responsible for the slowly decaying oscillatory response. There are also two of zeroes, one located at the origin and one on the real axis near the Nyquist frequency (see Fig. 3).

The proximity of the conjugate symmetric pair of poles to the unit circle indicates a slowly decaying sinusoidal oscillation. This effect is undesirable, as it slows down the rate at which the measurements can be made. If the measurement waveform interacts with still decaying previous output, accurate weight cannot be established. One way to avoid this is to use signal processing to reduce the transient response of the

$$H[z] = \frac{GB}{MR} \frac{z\left(\left(\frac{\sigma_A - \sigma_L}{\omega} r_L \sin\omega_0 - r_L \cos\omega_0 + r_A\right)z - r_L\left(\frac{\sigma_A - \sigma_L}{\omega} r_A \sin\omega_0 + r_A \cos\omega_0 - r_L\right)\right)}{(z - r_A)(z^2 - 2zr_L \cos\omega_0 + r_L^2)}, \qquad (14)$$

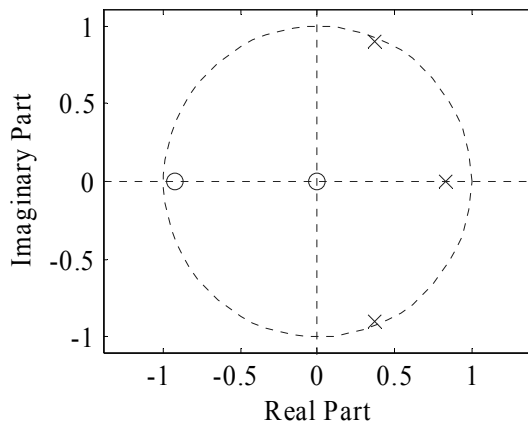where $r_A = e^{-\sigma_A T}$, $r_L = e^{-\sigma_L T}$, and $\omega_0 = \omega T$

Figure 3. Pole-zero map of the load cell-amplifier transfer function, with sampling rate of 500 Hz.
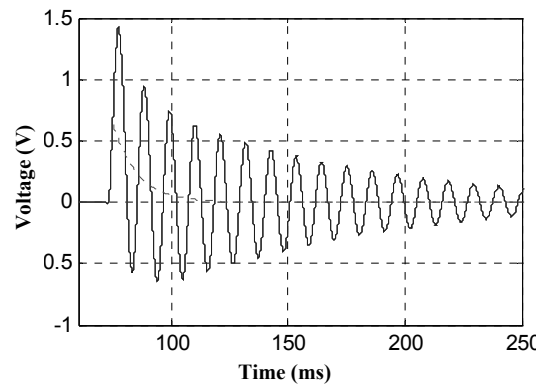

Figure 4. Example impulse response (Dashed line shows the exponential component due to the amplifier pole).

load cell. The exponential decay component of the impulse response due to the single real pole happen to have a much smaller time constant, as the pole is further away from the unit circle. Fig. 4 clearly shows that the exponential due to amplifier decays much faster than the decaying oscillations. This component of the impulse response can be used to determine the magnitude of the input impulse, if the oscillatory response is filtered out. Much faster decay rate allows making the measurements at a faster rate without any interference between consecutive measurements.

To reduce the effect of the conjugate symmetric poles, a pair of zeroes can be placed at the estimated position of the load cell poles. The second-order notch filter designed in this way is tuned specifically to filter out the slowly decaying periodic waveform produced by the resonating load cell.

The position of the load cell poles can be approximated from the frequency and the decay rate of the oscillation. A common method is to determine the frequency from the period of zero-crossings and the decay rate from the peaks. However, the first part of the waveform cannot be used for this, as it is "lifted" above the zero level by the second exponential. Only past the point where the second exponential is at negligible level, the zero-crossings can be utilized. Another method is to find troughs and crests and use the mid-points between two neighbouring troughs and crests in the same way as zero-crossings to determine the frequency. Both of these methods do not work very well in presence of noise and require a sampling rate considerably higher than the frequency of oscillation.

A better approach that has been investigated is to use a second order LMS adaptive filter [3] to track the position of the poles. With an appropriate step size the method showed good results and low noise susceptibility without requiring a high sampling rate.

Filtering leaves the fast-decaying impulse response of the amplifier at the output, which is proportional to the size of the initial impulse, shown in Fig. 5. The area of the impulse response (integrated impulse response) was used to determine the size of the impulse rather than the amplitude directly, as it is less susceptible to noise. The ripple before the peak and on the decaying side of the peak is Gibbs phenomenon due to the high frequency harmonics being filtered out by the decimation filter [4].

After the impulse response has decayed away, there can be seen a small ripple; it is due to a small misalignment in the position of load cell poles and filter zeroes. The ripple is insignificant and, as can be seen from Fig. 6, is hardly visible after integration.

The procedure used with the second amplifier was slightly different. It can be seen from Table I that the bandwidth of the second amplifier is much larger; therefore, the impulse response of this amplifier is very narrow relatively to the sampling frequency. Estimating the size of the impulse from this would give inaccurate results. Instead, a digital first order low pass filter, similar in characteristics to that of the first amplifier, was created. When the signal was passed through this filter, the result was very similar to the output that the first
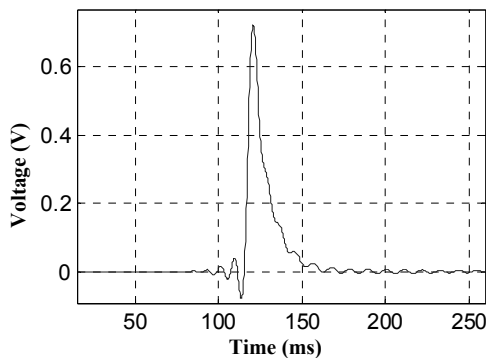

Figure 5. Slowly decaying periodic waveform has been filtered to show amplifier impulse response.
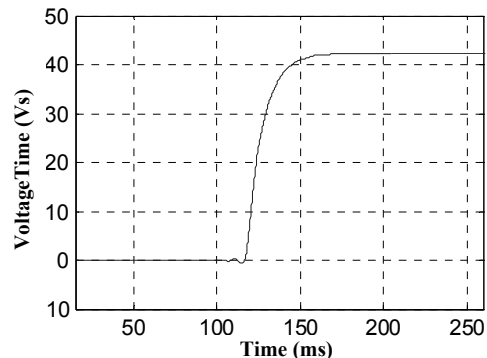

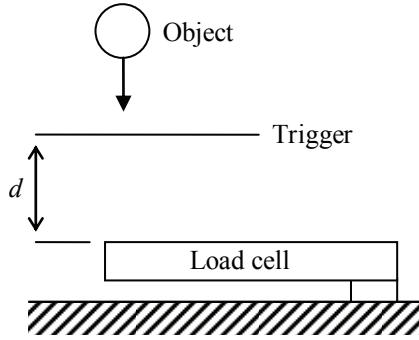Figure 6. Integration provides a more accurate result smoothing out left over ripple.

Figure 7. Side view: object breaks the trigger to start acquisition and a short time later collides with the load-cell.
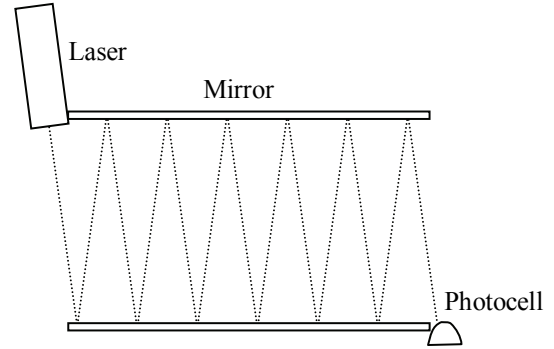

Figure 8. Top view: two mirrors, a laser, and a phototransistor are arranged to create a laser beam field above the load-cell.

amplifier would have produced. The impulse response of the filter enabled us to estimate the size of the impulse in the same way the impulse response of the first amplifier did. By controlling the cut frequency, it was possible to increase or decrease the time required to make a single measurement.

II. EXPERIMENTAL RESULTS

This section demonstrates experimentally the method of weighing described in previous section, with particular application to high-speed weighing.

A. Apparatus set-up

The apparatus set-up is quite simple. A load cell is mounted on top of a heavy steel base, as shown in Fig. 7. Around the load cell is a frame designed to hold two mirrors, a low-power laser, and a phototransistor. Mirrors are mounted in such a way that allows them to be rotated around vertical and horizontal axes. These are set up to create a uniform laser beam field between the mirrors, as pictured in Fig. 8. The laser beam field is positioned in the path of the falling objects, so that when an object is dropped onto the load cell, it breaks the beam, triggering the data acquisition card to start acquisition. The time between the trigger and the impact is used to calculate the impact velocity, as described in the previous section.

Steel balls with a range of diameters (and weights) were used as sample objects. The balls were dropped from various known heights in such a way, that they passed through the laser trigger before coming into contact with the load cell. Each measurement was repeated a number of times to gain some knowledge into the uncertainties involved.

1) Load Cell:
Two similar single-point bending beam anodised aluminium load cells were used to complete the experiment. As a precaution, an aluminium plate was attached to the top of the live end of each load cell to prevent any

damage to the load cell from impacts. This plate introduced additional damping to the system, shortening the time constant. As the aluminium plate was not sufficiently hard to sustain the forces generated during impacts without deformation, a thin layer of polymer plastic was glued to the top surface of the aluminium plate.

2) Instrumentation Amplifier:
Each load cell was used with its own amplifier. A1 was used with LC1 and was designed by RS Components. Unfortunately, its low bandwidth made it inappropriate for use with LC2, as the resonant frequency of LC2 is much higher. It is for this reason the second amplifier was designed and built. A2 has a much lower CMRR, due to absence of high precision matched components. Nevertheless, it was sufficient to demonstrate the principle.

Table I shows the important differences between the two load cells and amplifiers used in the experiment.

3) Software:
The acquisition software was written in LabVIEW 6.1 with digital filtering implemented in Matlab 6.5. The A National Instruments oscilloscope card was used in the experiment with LC1/A1. This card has a limited precision of 8 bits, which in theory limits the signal-to-noise ratio (SNR) to approximately 48 dB. In order to improve SNR, the signal was sampled at 50 kHz, then decimated and down-sampled to 500 Hz. This approach decreases the quantization noise power in the signal band of interest by approximately 20 dB, giving a total theoretical precision of approximately 11 bits. Downsampling has been performed in two steps in order to use a simpler decimation filter. First, an equiripple low pass filter was used with a transition band between 1000 and 1500 Hz. Then, the signal was downsampled by a factor of 10 to 5 kHz and a filter with the same coefficients was applied again. At this sampling frequency, the transition region was located between 100 and 150 Hz. Then, the signal was downsampled by another factor of 10 to 500 Hz.

In the second experiment a National Instruments PCI1200 acquisition card has been employed. This card has 12-bit quantisation. This was found to be sufficient and sampling at a much higher rate was not employed.

B. Impact Velocity Results

The results of the experiment indicate that there is a linear relationship between the measured size of the impulse J and the impact velocity of dropped objects.

TABLE I
PARAMETERS OF THE LOAD CELLS AND AMPLIFIERS USED IN THE EXPERIMENT

Parameter	LC 1 / A 1	LC 2 / A 2
load cell mass	200 g	600 g
plate mass	44 g	44 g
spring constant k_S	41 kN/m	3.5 MN/m
resonant frequency f	100 Hz	740 Hz
damping time constant τ	83 ms	45 ms
gain	1000	200
CMRR	>120 dB	60 dB
bandwidth	15 Hz	8 kHz
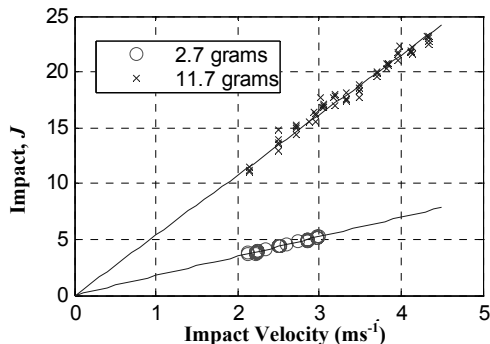
Figure 9.   Plot of impact J vs impact velocity for two constant weights.

Figure 10. Plot of normalized impact I vs mass with a least-squares fit.

Fig. 9 shows the plot of impact J against impact velocity v_m. It can be seen from the figure that the heavier mass has a larger relative error, which probably arises from the deformations during the impact.

C.   Weighing Results

Fig. 10 shows the result of a number of known weights dropped from different heights onto the LC2. The impact has been normalised by the impact velocity, to make it independent of the height: $I = J / v_m$. A least squares fit (using Gauss-Newton method) gave $M = 194$ grams. This compares well with the estimated mass of the load cell live end of 200 grams.

D.   High-speed Weighing Results

To demonstrate the concept of high-speed weighing, three almost identical in weight objects were dropped onto the load cell with about 250 ms separating the impacts. Fig. 11 shows the output of the load cell amplifier digitized at 50 kHz.

It is clear that the impulse responses produced by the three different impacts severely interfere with each other. After filtering and integration over 50 ms, the mass of each object can be estimated. Fig. 12 shows that a time interval of approximately 50 ms is required to make each measurement, giving a theoretical measurement rate as high as 20 measurements per second for the given amplifier.

III.   DISCUSSION AND CONCLUSIONS

The results have shown that the impact impulse on a load cell can be used to perform weight measurements. Signal processing can be used to extend this method to perform measurements at a much higher rate. However, a number of as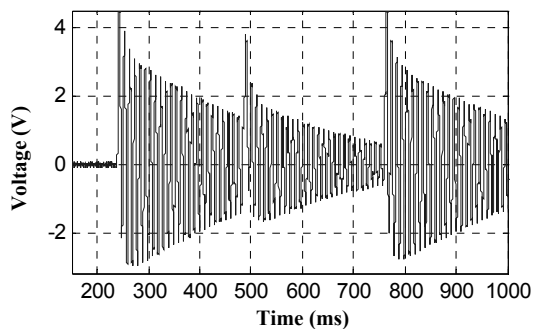sumptions have been made to simplify the analysis. These assumptions do not hold in a real system, introducing some uncertainty into the measurements. The most important is the assumption that the load cell velocity prior to the impact is zero. This is inherently wrong and as seen from Fig. 12 causes slight error – all three measurements should give the same result. The analysis will be extended in future work.

There are a number of limitations to this method, which follow from the conservation of linear momentum. Consider (11): the object will reverse its direction of travel after the impact, only if the mass of the object m is smaller than the product of the restitution coefficient and the equivalent mass of the load cell live end eM. If the object continues to travel in the same direction as before it will be struck again after half a cycle of the load cell oscillation. This will result in a second impulse, opposite in the direction to the first impulse, which will partially cancel out the effect of the first impulse.

There is also a trade-off between the rate of making measurements and the accuracy of the measurements. The area of the impulse response is used instead of the amplitude to compute the size of the impact impulse, as it is less susceptible to noise. Increasing the area by lowering the cut-off frequency of the amplifier/filter means higher signal-to-noise ratio. However, this also increases the time constant, decreasing the maximum rate of making measurements.

REFERENCES

[1]   J. Calpe, et al., "High-speed weighing system based on DSP", *IEEE 2002 28th Annual Conf. of the Industrial Electronics Society*, vol 2, pp. 1579-1583, November 2002.

[2]   G. E. Drabble, *Dynamics*. Macmillan Education Ltd, 1990.

[3]   P. Grant, C. Cowan, B. Mulgrew, and J. Dripps, *Analogue and Digital Signal Processing and Coding*. New York: Chartwell-Bratt Ltd, 1989.

[4]   Sanjit K. Mitra, *Digital signal processing : a computer-based approach*. New York: McGraw-Hill, 1998.

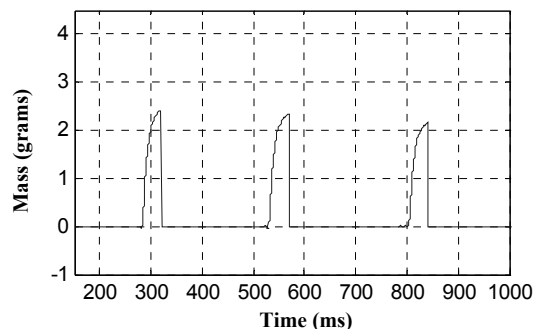Figure 11. Three impulse responses severely interfere.

Figure 12. After filtering and integration, three impacts can be clearly distinguished